Electronic Supplementary Material (ESI) for Journal of Materials Chemistry B.

A time-resolved ratiometric luminescent anthrax biomarker nanosensor based on Ir(III) complex-doped coordination polymer networks

Hui Zhang,‡[a] Meng Sun,‡[a] Ying Wang,[a] Li Yin,[a] Dik-Lung Ma,[b] Chung-Hang Leung[c] and Lihua Lu*[a]

[a] *College of Chemistry and Pharmaceutical Sciences, Qingdao Agricultural University, Qingdao 266109, China. E-mail: lulihua2012@qau.edu.cn.*

[b] *Department of Chemistry, Hong Kong Baptist University, Kowloon Tong, Hong Kong, China.*

[c] *State Key Laboratory of Quality Research in Chinese Medicine, Institute of Chinese Medical Sciences, University of Macau, Macao, China.*

‡ These authors contributed equally to this work.

Materials

Dipicolinic acid (DPA, 2,6-pyridinedicarboxylic acid, 99%) was purchased from TCI Co. Ltd., Guanosine 5′-monophosphate disodium (GMP, 98%) was bought from Sangon Biotech (Shanghai) Co. Ltd. Shanghai, China. Europium chloride ($EuCl_3 \cdot 6H_2O$, 99.9%) was purchased from Bailingwei Technology Co., Ltd., Beijing, China. All reagents were of analytical grade and used without further handling. Ultrapure water (resistivity > 18.2 ΩM·cm @ 25°C) was obtained from the Milli Q water purification system from the Millipore Company in Bedford, United States. Tris-HCl buffer (50 mM, pH = 9.0) was prepared by dissolving 605 mg Tris in 100 mL of deionized water, and the pH was calibrated by HCl using a pH meter (Sartorius AG, Germany).

Instruments and determinations

UV-visible absorption spectra were measured on a U-3900-VIS spectrophotometer with the scanning range of 200−700 nm. Fourier transform infrared spectra (FTIR) were recorded on a Perkin-Elmer Paragon 1000 infrared spectrometer in the range of 4000−399 cm^{-1}. Transmission electron microscopy (TEM) images were recorded on an HT-7700 microscope (Hitachi, Japan) operated at 100 kV. Zeta potential was recorded using a Zetasizer Nano ZS90 (Malvern Instruments, Malvern, UK). All steady state fluorescence spectra were obtained with a Hitachi F-7000 fluorescence spectrometer (Tokyo, Japan) at the excitation wavelength of 272 nm with the slit set of 5 nm, respectively.

Preparation of Ir(III) complex Ir(III)-2F

Ir(III)-2F was prepared according to the reported method[1]. Specifically, the intermediate Ir(III) complex dimer [Ir_2(2-(2,4-difluorophenyl)pyridine)$_4Cl_2$] was synthesized using the C^N ligand 2-(2,4-difluorophenyl)pyridine. A suspension of [Ir_2(2-(2,4-difluorophenyl)pyridine)$_4Cl_2$] (0.15 mmol) and corresponding N^N ligand (2, 2'-bipyridine) (0.15 mmol) were added in a mixture of DCM/methanol (1:1.2, 22 mL). The mixture was refluxed under the protection of nitrogen for 18 h. Then, a methanol solution of ammonium hexafluorophosphate (excess) was added into the gradual transparent reaction solutions dropwise. Afterwards, the mixture was distilled by rotary evaporation until a precipitation appeared. The crude product was received through filtering and washing the precipitation with several portions of water and diethyl ether. Finally, the target Ir(III)-2F was obtained through the recrystallization in acetonitrile/diethyl ether. The ^1H NMR, ^{13}C NMR and HRMS of complex **1** was consistent with the reported one.

Preparing Ir(III)@GMP-Eu^{3+} in one pot

Ir(III) complex is named as Ir(III)-2F, which was synthesized according to the reported method[1]. Its specific preparation process is presented in the part of electronic supporting information (ESI). To prepare Ir(III)@GMP-Eu^{3+} CPNs, firstly, 6.0 mL GMP (10 mM) aqueous solution and 3.0 mL Ir(III)-2F (1 mM) methanol solution were mixed and stirred for 30 min. Afterwards, 6.0 mL $EuCl_3$ (10 mM) aqueous solution was put into the mixture and stirred for 1.5 h at 25 °C. Then, the reaction solution was centrifuged at 8,000 rpm for 10 min, and the precipitates were washed with ultra-pure water for several times to remove the unreacted reagents. Lastly, Ir(III)@GMP-Eu^{3+} was resuspended in pure water with the concentration of 1 $mg \cdot mL^{-1}$ for after using.

Detecting DPA in buffered solution with steady state emission spectrum (SSES)

30 μL as-prepared Ir(III)@GMP-Eu^{3+} (1 $mg \cdot mL^{-1}$) was added in 60 μL Tris-HCl (50 mM, pH =7) buffer[2]. Then, 10 μL DPA with different concentrations (0, 0.01, 0.025, 0.05, 0.1, 0.2, 0.3, 0.5, 0.8, 1, 2, 3, 4 , 5, 6, 7 and 8 μM) were put into the nanoprobe solution. After 1 min, the luminescent spectra were tested under the excitation at 272 nm.

Different organic acids, including glutamic acid (Glu), cysteine (Cys), *p*-phthalitic acid (p-Ph), phthalitic acid (Ph), *l*-asparaginic acid (Asp), phenylanine (Phe) and alanine (Ala) were chosen as the interferences to investigate the selective of the nanosensor. The interference experiment was performed in the mixtures of DPA with other organic acids. The final concentration of those substances were 10 μM, and the DPA was 5 μM.

Monitoring DPA in 10% human serum through TRES

Firstly, 30 μL as-prepared Ir(III)@GMP-Eu^{3+} (1 $mg \cdot mL^{-1}$), 50 μL Tris-HCl (50 mM, pH =7) buffer and 10 μL human serum were added in a 100 μL cuvette, then, 10 μL DPA with different concentrations (0, 1, 2, 3, 4 and 5 μM) were put into the nanoprobe-contained solution. Lastly, TRES was carried out using a Horiba Fluorolog TCSPC spectrophotometer (FLS1000, excitation: 295 nm; time range: 0–18 μs; time interval: 80 ns; wavelength interval: 10 nm).

Imaging spores' germination

Firstly, the third-generation *Bacillus subtilis* was cultured on a slant medium for about 10 days[3]. Then, the spores were centrifuged at 5800 rpm for 12 min and subsequently

washed with ultrapure water for three times. After removing supernatant, the purified spores (1.5×10^9 CFU·mL^{-1}) were re-dispersed in sterile deionized water. To promote spores germinate, the stored spores suspension was diluted 10-fold and keeped at 90 °C for 25 min. Then, dodecylamine solution (2 mM, 10 μL) was put into the processed spores solution (90 μL) and incubated with Ir(III)@GMP-Eu^{3+} (100 μL) solution immediately. Then, the varies of the phosphorescence intensity were monitored under the emission inverted microscope every few minutes.

Optimizing the contents of Ir(III)@GMP-Eu^{3+}

To optimize the content of Ir(III)@GMP-Eu^{3+} CPNs, 6.0 mL GMP with different concentrations (5, 10,15, 20 and 25 mM) aqueous solution and 3.0 mL Ir(III)-2F (1 mM) methanol solution were mixed and stirred for 30 min. Afterwards, 6.0 mL $EuCl_3$ (10 mM) was put into the mixture and stirred for 1.5 h at 25 °C. Then, the after steps are the same as that of DPA detection in buffered solution.

Monitoring the interaction time between Ir(III)@GMP-Eu^{3+} with DPA

To monitor the interaction time between Ir(III)@GMP-Eu^{3+} with DPA, the scan wavelength range is set up as 610−625 nm. Then the sample containing 1 mg·mL^{-1} Ir(III)@GMP-Eu^{3+} and 5 μM DPA was tested every 5 s under the excitation at 272 nm.

Table S1 Other DPA detection methods reported in recent literatures

Methods	**Detection limit**	**Linear range**	**Reference**
A time-resolved ratiometric luminescent anthrax biomarker nanosensor based on an Ir(III) complex-doped coordination polymer networks	3.3 nM	0.005−5 μM	This work
A ratiometric fluorescent probe for determination of the anthrax biomarker 2,6-pyridinedicarboxylic acid based on a terbium(III)-functionalized UIO-67 metal-organic framework	36 nM	0.3−6 μM	[4]
Europium functionalized silicon quantum dots nanomaterials for ratiometric fluorescence detection of bacillus anthrax biomarker	1.02 μM	0−34 μM	[5]
Ratiometric fluorescent detection of biomakers for biological warfare agents with carbon dots chelated europium-based nanoscale coordination polymers	5.1 nM	0.025−5 μM	[6]

BSA-AuNPs@Tb-AMP metal-organic frameworks for ratiometric fluorescence detection of DPA and Hg^{2+}	17.4 nM	0.05−10 μM	[7]
Ratiometric fluorescence detection of 2,6-pyridine dicarboxylic acid with a dual-emitting lanthanide metal-organic framework (MOF)	1087 nM	0−1 μM	[8]
In situ incorporation of fluorophores in zeolitic imidazolate framework-8 (ZIF-8) for ratio-dependent detecting a biomarker of anthrax spores	67 nM	0.1−150 μM	[9]
A Eu^{3+}-inspired fluorescent carbon nanodot probe for the sensitive visualization of anthrax biomarker by integrating EDTA chelation	190 pM	1−100 nM	[10]
Dual lanthanide-doped complexes: the development of a time-resolved ratiometric fluorescent probe for anthrax biomarker and a paper-based visual sensor	7.3 nM	0.05−2 μM	[11]
A ratiometric fluorescence visual test paper for an anthrax biomarker based on functionalized manganese-doped carbon dots	0.1 nM	0.1−750 nM	[12]
Screen-printed fluorescent sensors for rapid and sensitive anthrax biomarker detection	0.5 nM	0.1−100 nM	[13]
Luminescent AuNPs@Tb/adenosine monophosphate nanostructures for 2, 6-pyridinedicarboxylic acid detection	2.7 nM	0.01−10 μM	[14]
A nanoscaled lanthanide metal-organic framework as a colorimetric fluorescent sensor for dipicolinic acid based on modulating energy transfer	4.55 nM	50−700 nM	[15]
Rapid and facile ratiometric detection of an anthrax biomarker by regulating energy transfer process in bio-metal-organic framework	34 nM	0.05−1 μM	[16]
Fluorescent europium-modified polymer nanoparticles for rapid and sensitive anthrax sensors	10 pM	0.1−100 nM	[17]
Portable smartphone platform integrated with fluorescent test strip based on Eu^{3+}-functionalized copper nanoclusters for on-site visual recognition of a pathogenic biomarker	8 nM	0−20 μM	[18]

Europium-decorated ZnO quantum dots as fluorescent sensor for the detection of anthrax biomarker	3 nM	0.004−4 μM	[19]
Nanoscaled lanthanide/nucleotide coordination polymer for detection of an anthrax biomarker	10 nM	0.02−20 μM	[20]
Dual-emission of silicon nanoparticles encapsulated lanthanide-based metal-organic frameworks for ratiometric fluorescence detection of bacterial spores	5.3 nM	0.025−3 μM	[21]
A ratiometric lanthanide-free fluorescent probe based on two-dimensional metal-organic frameworks and carbon dots for the determination of anthrax biomarker	7 nM	0.2−10 μM	[22]
A luminous off-on probe for the determination of 2,6-pyridinedicarboxylic acid as an anthrax biomarker based on water-soluble cadmium sulfide quantum dots	0.2 μM	1−120 μM	[23]
Stimulus response of TPE-TS@Eu/GMP ICPs: toward colorimetric sensing of an anthrax biomarker with double ratiometric fluorescence and its coffee ring test kit for point-of-use application	27 nM	0.08−40 μM	[24]

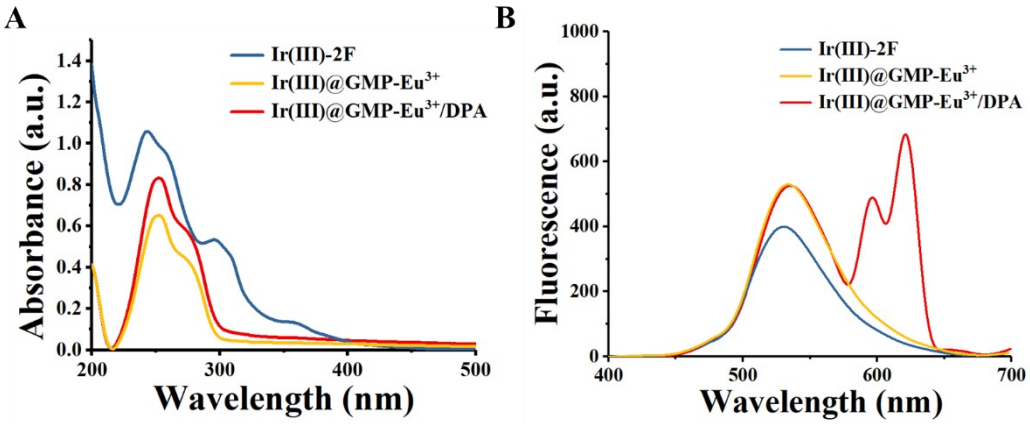

Fig. S1 (A) UV-Vis absorption spectra of Ir(III)-2F, Ir(III)@GMP-Eu^{3+} and Ir(III)@GMP-Eu^{3+}/DPA. (B) The emissions of Ir(III)-2F, Ir(III)@GMP-Eu^{3+} and Ir(III)@GMP-Eu^{3+}/DPA

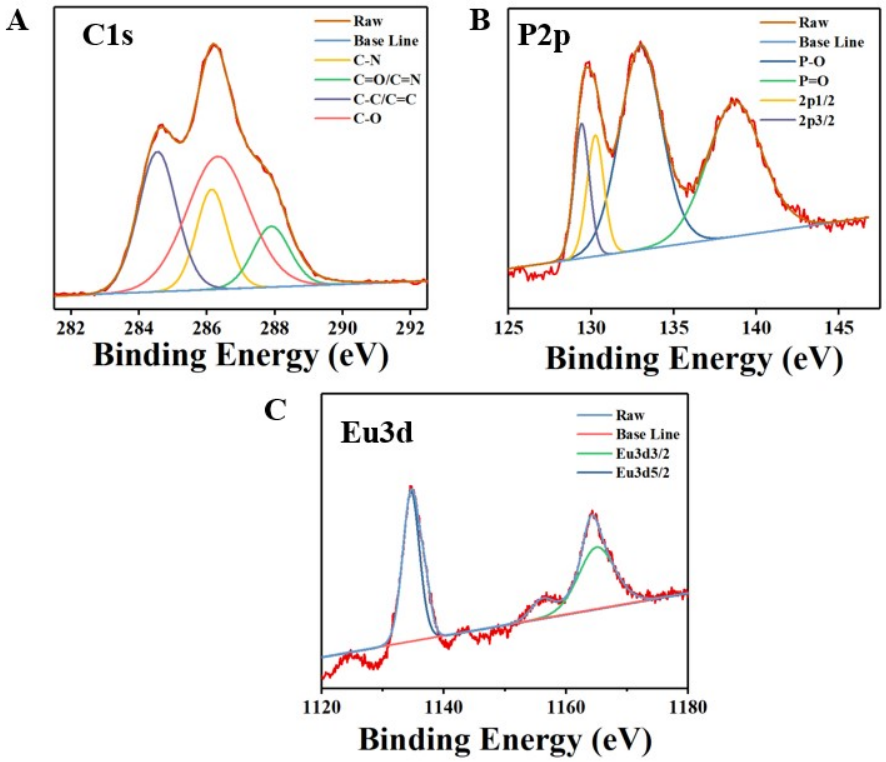

Fig. S2 High resolution XPS spectra of (A) C 1s (B) P 2p and (C) Eu 3d

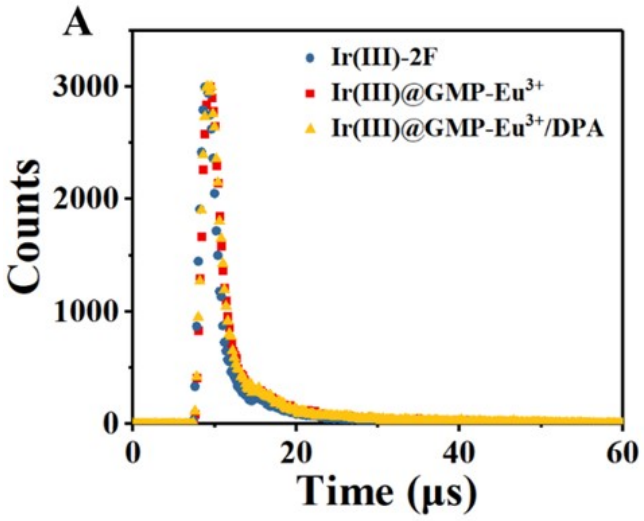

Fig. S3 The time-resolved phosphorescence decay spectra of Ir(III)-2F, Ir(III)@GMP-Eu^{3+} and Ir(III)@GMP-Eu^{3+}/DPA at 525 nm

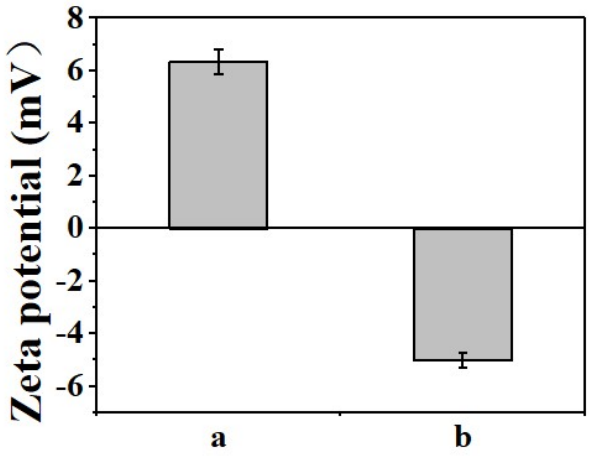

Fig. S4 The Zeta-potential of (a) Ir(III)@GMP-Eu^{3+} and (b) Ir(III)@GMP-Eu^{3+}/DPA

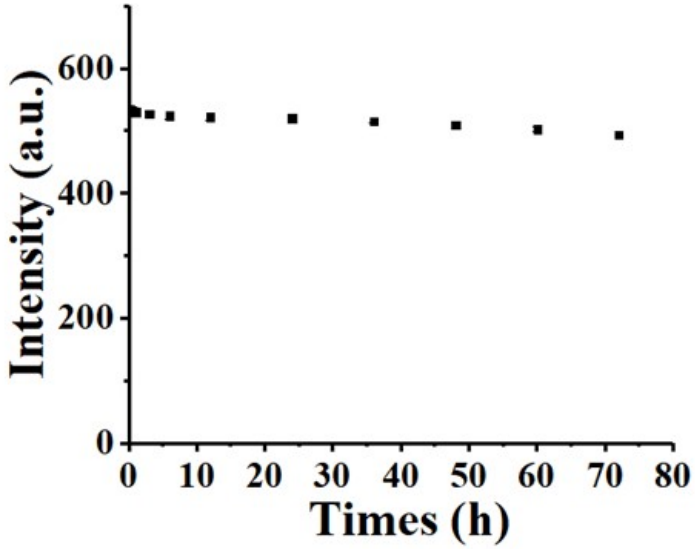

Fig. S5 Luminescence intensities of Ir(III)@GMP-Eu^{3+} (1 mg·mL^{-1}) corresponds to different times in buffered solution

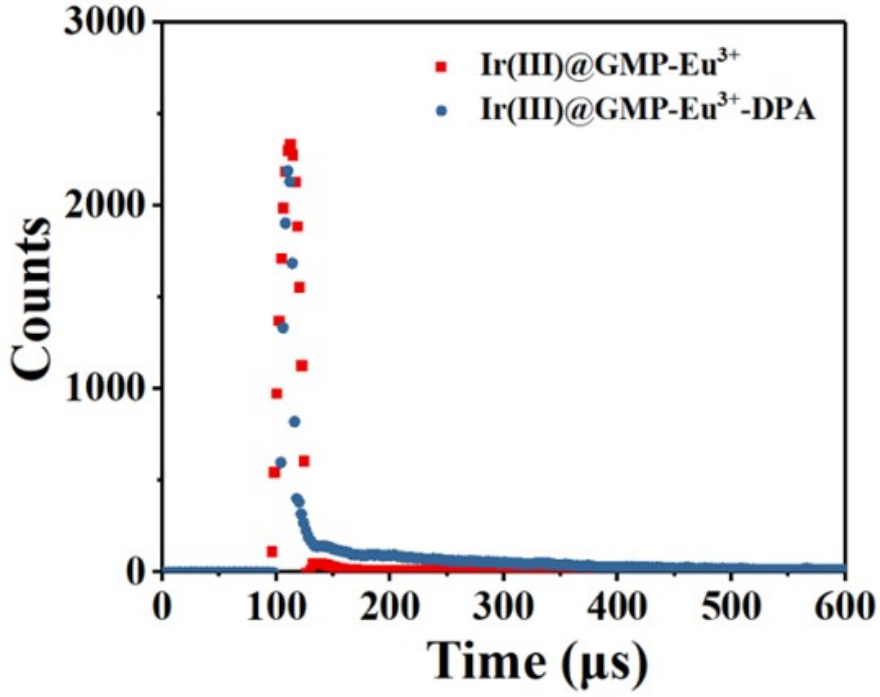

Fig. S6 The time-resolved phosphorescence decay spectra of Ir(III)@GMP-Eu^{3+} and Ir(III)@GMP-Eu^{3+}/DPA at 620 nm

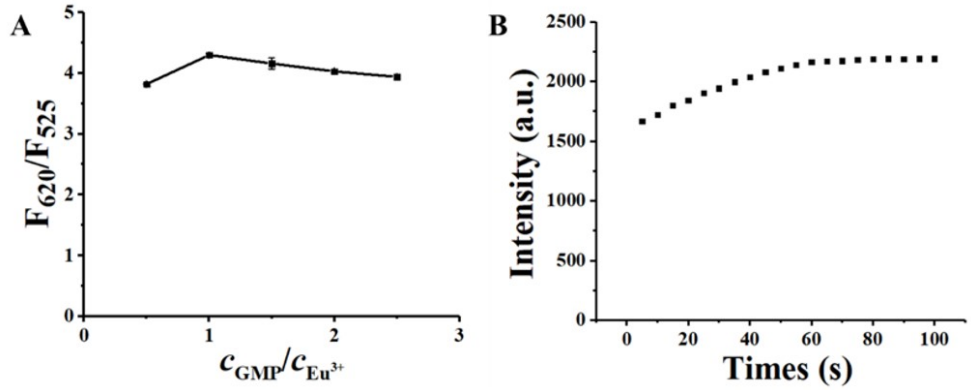

Fig. S7 (A) Relative intensities (F_{620}/F_{525}) of Ir(III)@GMP-Eu^{3+} corresponds to the concentration ratio of GMP with Eu^{3+}, (B) the fluorescence intensity of Ir(III)@GMP-Eu^{3+} at λ_{em}= 620 nm towards interaction time

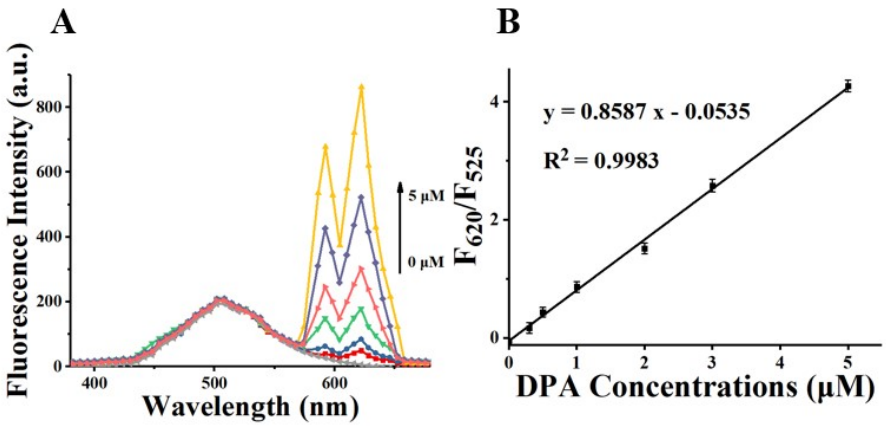

Fig. S8 (A) The TRES of the DPA (0, 0.3, 0.5, 1, 2, 3 and 5 μM) detection system in buffered solution. (B) Linear plot of the F_{620}/F_{525} value corresponds to DPA concentrations (0, 0.3, 0.5, 1, 2, 3 and 5 μM) in TRES

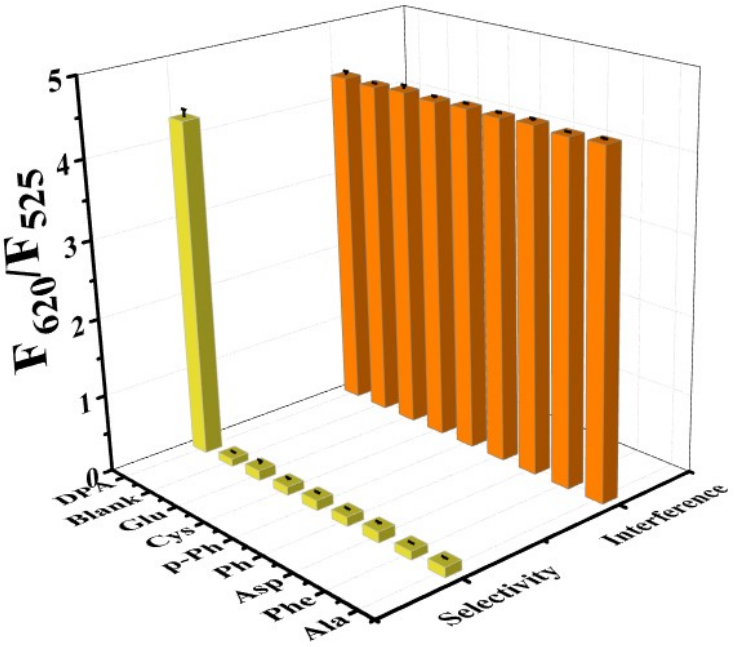

Fig. S9 Relative intensities (F_{620}/F_{525}) of Ir(III)@GMP-Eu^{3+} in the presence of various organic acids, or their mixtures with DPA (The concentration of DPA is 5 μM, and the concentrations of other organic acids are 10 μM)

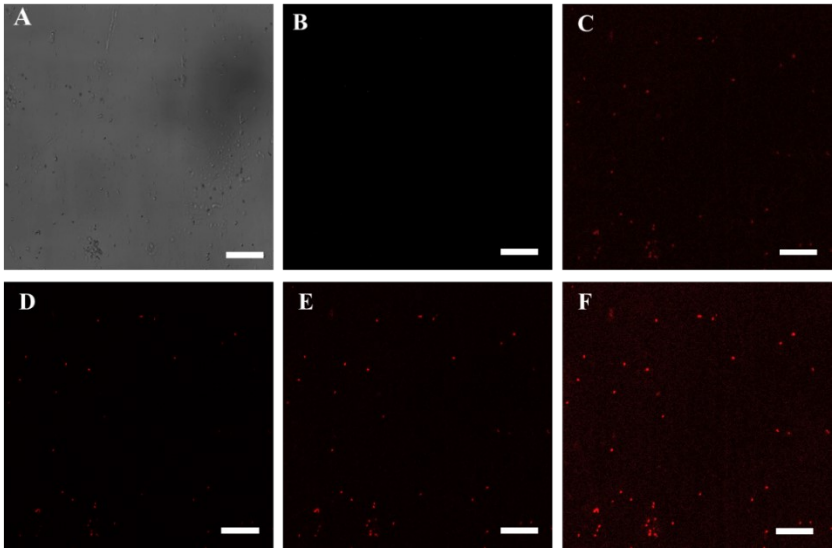

Fig. S10 (A) Bright field microscopy images of Ir(III)@GMP-Eu^{3+} incubated with spores. (B) Luminescence microscopy imaging of Ir(III)@GMP-Eu^{3+} incubated with ungerminated spores (without DOD) in red channel. (C) Luminescence microscopy imaging of Ir(III)@GMP-Eu^{3+} incubated with spores germinated (with DOD) after 5 min, 10 min, (D), 20 (E) and 30 min (F) in red channel, respectively. Scale bar is 100 μm

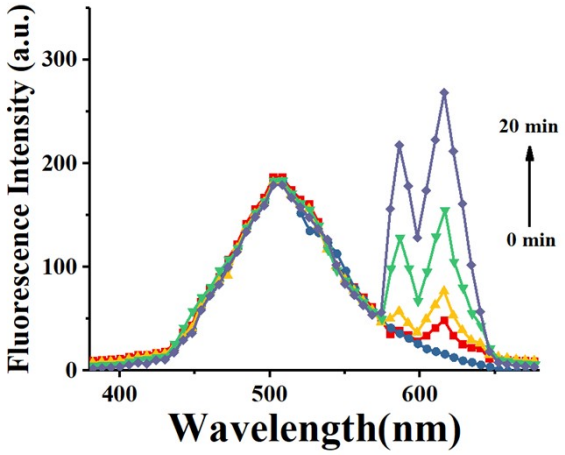

Fig. S11 The germination process (0, 5, 10 and 15 min) of B. subtilis spores monitored by TRES

Reference

1. J.S. Nam, M.G. Kang, J. Kang, S.Y. Park, S. Lee, H.T. Kim, J.K. Seo, O.H. Kwon, M.H. Lim, H.W. Rhee. Endoplasmic reticulum-localized iridium(III) complexes as efficient photodynamic therapy agents via protein modifications[J]. J Am Chem Soc, 2016, 138 : 10968.

2. Y. Song, J. Chen, D. Hu, F. Liu, L. Ping, H. Li, S. Chen, H. Tan, W. Li. Ratiometric fluorescent detection of biomakers for biological warfare agents with carbon dots chelated europium-based nanoscale coordination polymers[J]. Sens Actuators B Chem, 2015, 221:586-92.
3. M. Yilmaz, H.A. Oktem. Eriochrome Black T-Eu^{3+} complex as a ratiometric colorimetric and fluorescent probe for the detection of dipicolinic acid, a biomarker of bacterial spores[J]. Anal Chem, 2018, 90:4221-4225.
4. X. Zhang, W. Zhang, G. Li, Q. Liu, Y. Xu, X. Liu. A ratiometric fluorescent probe for determination of the anthrax biomarker 2,6-pyridinedicarboxylic acid based on a terbium(III)− functionalized UIO-67 metal-organic framework[J]. Microchim Acta, 2020, 187(2):122.
5. Z. Zhou, J. Gu, Y. Chen, X. Zhang, H. Wu, X. Qiao. Europium functionalized silicon quantum dots nanomaterials for ratiometric fluorescence detection of Bacillus anthrax biomarker[J]. Spectrochim Acta, Part A, 2018, 18：31106.
6. Song, Chen, Hu, Liu, Li, Li, Chen, Tan, Wang. Ratiometric fluorescent detection of biomakers for biological warfare agents with carbon dots chelated europium-based nanoscale coordination polymers[J]. Sens Actuators B Chem, 2015, 221:586-92.
7. K. Cai, M. Zeng, F. Liu, N. Liu, Z. Huang, Y. Song, L. Wang. BSA–AuNPs@Tb–AMP metal–organic frameworks for ratiometric fluorescence detection of DPA and Hg^{2+}[J]. Luminescence, 2017, 32: 1277-82.
8. M. Wu, Y. Zhuang, J. Liu, W. Chen, R.J. Xie. Ratiometric fluorescence detection of 2,6-pyridine dicarboxylic acid with a dual-emitting lanthanide metal-organic framework (MOF)[J]. Opt Mater, 2020, 106:110006.
9. X. Li, J. Luo, L. Deng, F. Ma, M. Yang, In situ incorporation of fluorophores in zeolitic imidazolate framework-8 (ZIF-8) for ratio-dependent detecting a biomarker of anthrax spores, Anal Chem, 2020, 92: 7114-7122.
10. H. Yang, F. Lu, X. Zhan, M. Tian, Z. Yuan, C. Lu. A Eu^{3+} -inspired fluorescent carbon nanodot probe for the sensitive visualization of anthrax biomarker by integrating EDTA chelation[J]. Talanta, 2020, 208:120368.
11. Q.X. Wang, S.F. Xue, Z.H. Chen, S.H. Ma, S. Zhang, G. Shi, M. Zhang. Dual lanthanide-doped complexes: the development of a time-resolved ratiometric fluorescent probe for anthrax biomarker and a paper-based visual sensor[J]. Biosens Bioelectron, 2017, 94: 388-93.
12. M. Rong, Y. Liang, D. Zhao, B. Chen, C. Pan, X. Deng, Y. Chen, J. He. A ratiometric fluorescence visual test paper for an anthrax biomarker based on functionalized manganese-doped carbon dots[J]. Sens Actuators B Chem, 2018, 265: 498-505.
13. I. Lee, W.K. Oh, J. Jang. Screen-printed fluorescent sensors for rapid and sensitive anthrax biomarker detection[J]. J Hazard Mater, 2013, 252:186-191.
14. M. Zeng, F. Liu, H. Dong, J. Hao, P. Li, L. Wang, Z. Huang, Y. Song. Luminescent AuNPs@Tb/adenosine monophosphate nanostructures for 2,6-pyridinedicarboxylic acid detection[J]. Anal Methods, 2016, 8: 3892-8.

15. Y. Zhang, B. Li, H. Ma, L. Zhang, H. Jiang, H. Song, L. Zhang, Y. Luo. A nanoscaled lanthanide metal–organic framework as a colorimetric fluorescence sensor for dipicolinic acid based on modulating energy transfer[J]. J Mater Chem C, 2016, 4: 7294-301.
16. Y. Zhang, B. Li, H. Ma, L. Zhang, Y. Zheng. Rapid and facile ratiometric detection of an anthrax biomarker by regulating energy transfer process in bio-metal-organic framework[J]. Biosens Bioelectron, 2016, 85: 287-93.
17. W.K. Oh, Y.S. Jeong, J. Song, J. Jang. Fluorescent europium-modified polymer nanoparticles for rapid and sensitive anthrax sensors[J]. Biosens Bioelectron, 2011, 29 (1):172-177.
18. J. Zhao, Y. Chen, P. Du, J. Li, X. Lu. Portable Smartphone Platform Integrated with Fluorescent Test Strip Based on Eu^{3+}-functionalized Copper Nanoclusters for On-Site Visual Recognition of a Pathogenic Biomarker[J]. Sens Actuators B Chem, 2021, 332: 129495.
19. R. Zhou, Y. Zhao, Q. Liu, K. Dong. Europium-decorated ZnO quantum dots as a fluorescent sensor for the detection of an anthrax biomarker[J]. J Mater Chem C, 2017, 5 1685-1691.
20. F. Xu, L. Chen, C. Ma, L. Wang, S. Chen. Nanoscaled lanthanide/nucleotide coordination polymer for detection of an anthrax biomarker[J]. Sens Actuators B Chem, 2014, 190: 621-626.
21. D. Yang, S. Mei, Z. Wen, X. Wei, R. Guo. Dual-emission of silicon nanoparticles encapsulated lanthanide-based metal-organic frameworks for ratiometric fluorescence detection of bacterial spores[J]. Microchim Acta, 2020, 187 (12):666.
22. J. Bao, J. Mei, X. Cheng, D. Ren, Y. Cen. A ratiometric lanthanide-free fluorescent probe based on two-dimensional metal-organic frameworks and carbon dots for the determination of anthrax biomarker[J]. Microchim Acta, 2021, 188(3):84.
23. X. Li, L. Deng, F. Ma, M. Yang. A luminous off-on probe for the determination of 2,6-pyridinedicarboxylic acid as an anthrax biomarker based on water-soluble cadmium sulfide quantum dots[J]. Microchim Acta 2020, 187 (5):287.
24. C. Huang, R. Ma, Y. Luo, G. Shi, J. Deng, T. Zhou. Stimulus response of TPE-TS@Eu/GMP ICPs: toward colorimetric sensing of an anthrax biomarker with double ratiometric fluorescence and its coffee ring test kit for point-of-use application[J]. Anal Chem, 2020, 92 (19):12934-42.